Scientific Research Publishing

Materials Sciences and Applications, 2026, 17(4), 89-100
https://www.scirp.org/journal/msa
ISSN Online: 2153-1188
ISSN Print: 2153-117X

Synthesis and Characterization of Cu-Co-Mn Alloys for Aeronautic Applications: Microstructural and Mechanical Performance

Rene Guardia-Tapia[1], Juan Antonio Ruiz-Ochoa[2], Isai Rosales-Cadena[1*]

[1]Center for Research in Engineering and Applied Sciences CIICAp, Autonomous University of Morelos State, Cuernavaca, Mexico
[2]Faculty of Sciences of the Enginery and Technology, Universidad Autónoma de Baja California, Tijuana, Mexico
Email: *faye12@uaem.mx

How to cite this paper: Guardia-Tapia, R., Ruiz-Ochoa, J.A. and Rosales-Cadena, I. (2026) Synthesis and Characterization of Cu-Co-Mn Alloys for Aeronautic Applications: Microstructural and Mechanical Performance. *Materials Sciences and Applications*, **17**, 89-100.
https://doi.org/10.4236/msa.2026.174007

Received: February 17, 2026
Accepted: March 30, 2026
Published: April 2, 2026

Abstract

Cu-Co alloys with different manganese contents, were synthetized using the induction melting technique. Thermal treatments were applied to the resultant alloys, obtaining minimum superficial porosity. Scanning electron microscopy reveals a copper rich matrix and a secondary phase constituted of Mn-Co with precipitates mainly thorough the grain boundaries. Hardness evaluation shows average values for samples thermal treated of 138 HV which represent 12% lower than untreated samples, produced by the homogenization of the microstructure. Tribological analyses indicated that samples thermal treated have reached a noticeable increment in their wear resistance under an oxidative wear mechanism which make it as a promissory alloy for aeronautical applications.

Keywords

Structural Alloys, Hardness, Mechanical Properties, Wear

1. Introduction

Copper-manganese alloys with mechanical properties superior to the conventional aluminum alloys used in the aeronautical industry can be of great interest nowadays to fabricate resistant but ductile components. There is limited information related with the mechanical properties of this kind of alloys. S. Zuo [1] studied the orientation dependence of damping behavior in a Mn-Cu shape memory alloy in different crystal orientations by applying tensile stress. W. You [2] analized the effect of semi-solid solution and aging on microstructure and properties of Mn-Cu alloy showing that the microstructure of solid solution

treated alloy is composed of a single γ-MnCu phase, while that of the semi-solid solution treated may contain Mn-rich and Mn-poor γ-MnCu phases. Other authors studied the Mn-Cu alloys using different obtaining methods [3]-[6]. C. Ma [7] reported the effects of solution aging on the microstructure, phase transformation and mechanical properties of MnCuNiFe alloys reporting that increasing solution temperatures enhances the mechanical resistance and ductility of the alloy. Also relative new technologies such as laser engineering net shaping system and directed energy deposition has been applied to produce Mn-Cu alloys [8] [9]. K. Tsuchiya [10] investigated the aging response of shape memory behavior in γ-MnCu alloys and S. Shi [11] reported a thermodynamic study on Mn-Ni antiferromagnetic shape memory alloys. Other authors have worked on the analyses of phase transformations of Mn-Cu alloys from the microstructural point of view [12]-[14]. Several works have been developed based on the Mn-Cu system, evaluating the mechanical properties, phase transformations with the additions of different elements as reinforcement [15] [16], inclusive, the incorporation of rare earth elements [17]. This Cu-Co-Mn alloy is proposed as structural alloy due to the expected ductility offered by copper, together with the hardness provided by cobalt and manganese, with the finality to obtain structural components. Therefore, this paper present an extensive investigation of Cu-Co-Mn alloys, focusing on the design, synthesis and characterization of the alloy, from the microstructural and mechanical point of view, to generate complete information of these Cu-Co-Mn alloys, furthermore to provide a direction of the thermal treatment used to improve its microstructure for developing advanced materials. This paper also generates information of the tribological behavior based in the relationship between microstructure and hardness to obtain the best performance of these Cu-Co-Mn alloys to be used in different aeronautics applications in parts exposed to a constant friction (structural load-bearing components).

2. Experimental Procedure

Alloys containing different concentrations of Copper, Cobalt and Manganese (99.99%) were synthesized using an induction melting unit (see **Table 1** for alloy designation and composition). Alloys were melted using quartz crucibles under a vacuum atmosphere in chamber of 10^{-2} torrs. Thermal treatments were conducted by heating the samples to 500˚C for 15 minutes, followed by water quenching and a second heating treatment at 180˚C for 2 hours was applied, followed by air cooling to complete the ageing treatment. Cubic specimens (1 × 1 × 1 cm) were cut and prepared by sanding up to 600 grit, followed by polishing with 0.03 μm alumina (Al_2O_3) paste. The samples were etched for 20 seconds using 12.5 $FeCl_3$, 12.5 mL HCl, 50 mL distilled water. Microstructural characterization was performed using a Leo VP450 scanning electron microscope (SEM), Porosity measurements were performed using the IPA (Image Processing Analysis) software of the equipment by measuring the area fraction of the superficial area. Microhardness measurements were carried out on the polished surfaces using the Vickers method,

with a 0.1 kg load and a dwell time of 15 s, on a Leco 300 MT microhardness tester.

Wear evaluations were carried out using cylindrical samples (6 mm diameter × 8 mm length), tested under a rotational speed of 200 rpm, with zero lubrication, using a conventional pin-on-disk wear machine, applying a constant load of 0.5 kg and a sliding distance of 4 km. An AISI 4140 steel disk (oil quenched, 51 ± 3 HRC) was used as the counterpart. Worn surfaces were analyzed by SEM to dilucidate the wear mechanisms.

Table 1. Average grain size of the samples with heat treatment and without thermal treatment and porosity measurements average.

Alloy designation	Elemental composition [wt. %]			Average grain size [μm]	Porosity [%]
	Cu	Co	Mn		
M1	70	30	0	193.2	4.12
M2	70	25	5	131.28	3.83
M3	70	20	10	102.2	3.34
M1TT	70	30	0	129.5	4.25
M2TT	70	25	5	106.6	3.94
M3TT	70	20	10	85.4	3.42

3. Results and Discussions

3.1. Microstructural Analyses

The microstructure obtained from the surface of the M1 sample, thermal treated is shown in Figure 1, where, in zone 1 are observed enlarged second phases with a different length, while zone 2 exhibits a considerable amount of precipitates distributed within the matrix, with an average of 85 % of area fraction.

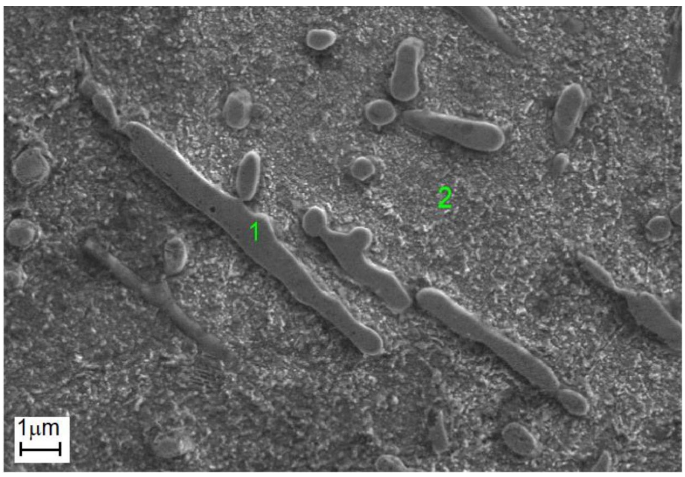

Figure 1. Microstructure of sample M1 with heat treatment showing the position of the two main phases precipitated.

The surface sample of M2 sample thermal treated is shown in Figure 2, where

it can be observed a columnar dendritic structure with precipitation of second phases with sizes of 15 μm average. The significant changes in the second phase shape and size are related to the solidification mechanisms of the alloys. It is well known that Mn presence as an alloying element may contributes to produce a grain and particle size refinement [18]. Here the area fraction of matrix result to be approximately of 75% which can be an important factor in the alloy strengthening.

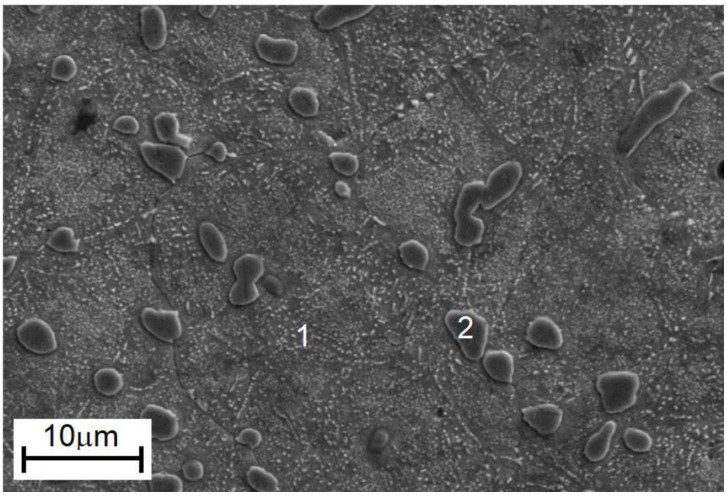

Figure 2. Microstructure of the heat-treated Cu-Co-Mn alloy showing the two phases precipitated.

Figure 3 shows the microstructure of M3 sample with thermal treatment applied, where it can be observed a great amount of second phases precipitated on the surface sample.

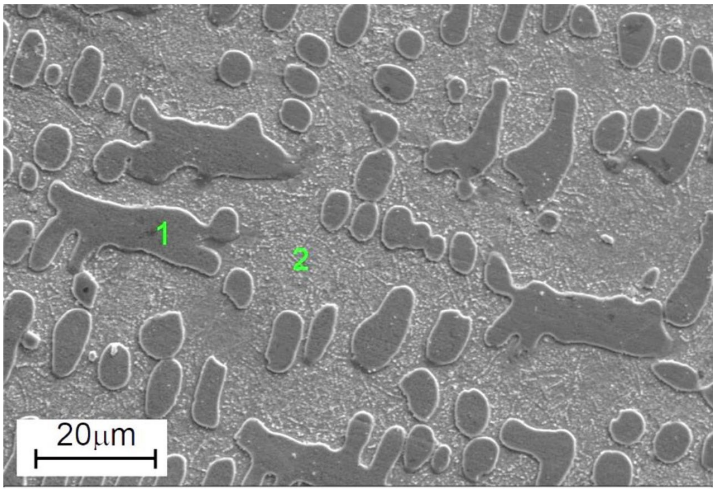

Figure 3. Microstructure of M3 sample with thermal treatment applied, showing the position of the two phases precipitated.

In zone 1, it can be observed that the second phase present the major area frac-

tion, but their growth is restricted in certain directions due to the formation adjacent second phases, this accumulation leads to an anisotropic growth of the phases, which eventually transform into larger structures, furthermore, surface energy and interfacial energy developed on the interface between the second phases and matrix, are the necessary parameters to transform a semi-coherent to a coherent structure. This applied thermal treatment, produce also a free internal thermal stress structure [18]. On the other hand, precipitation strengthening in copper alloys, is one of the main strengthening mechanism, where, in this case, these second phases are randomly distributed, working as obstacles that inhibit dislocation movement, which may improve the mechanical properties of the alloy [18]. The area fraction of matrix in this sample is of approximately 48%.

In order to determine the elements' position in the alloys, in **Figure 4**, the corresponding EDX elemental mapping of the element distribution of the M3 sample thermal treated is presented, where is clearly observed that manganese is segregated within the copper matrix and is also observed in the dendrite's surrounding contour, while Co is present in the dendrite's interior. This confirms that in the alloy the second phase is mainly composed of cobalt, although this result does not exclude the possibility that copper and a small amount of manganese can be present in this phase.

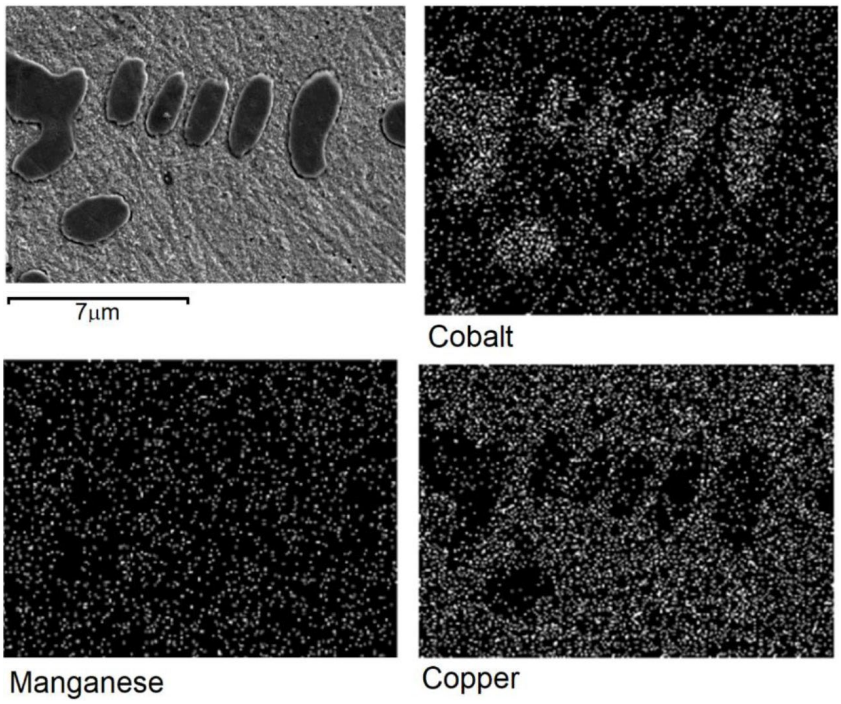

Figure 4. Elemental mapping on the surface of M3 sample, showing a second phase rich in Cobalt mainly.

In **Figure 5**, is presented the linear elemental analysis across two precipitates found in M3 sample thermally treated, showing the composition of Co, Mn, Cu, which is consistent with the distribution of elements shown in **Figure 4**. It can also

be observed that the precipitate has a high Co content, and the square-shaped precipitate has a high concentration of Mn, as can be observed in the linear chemical analysis, while Cu is observed with more intensity along the surface of the matrix.

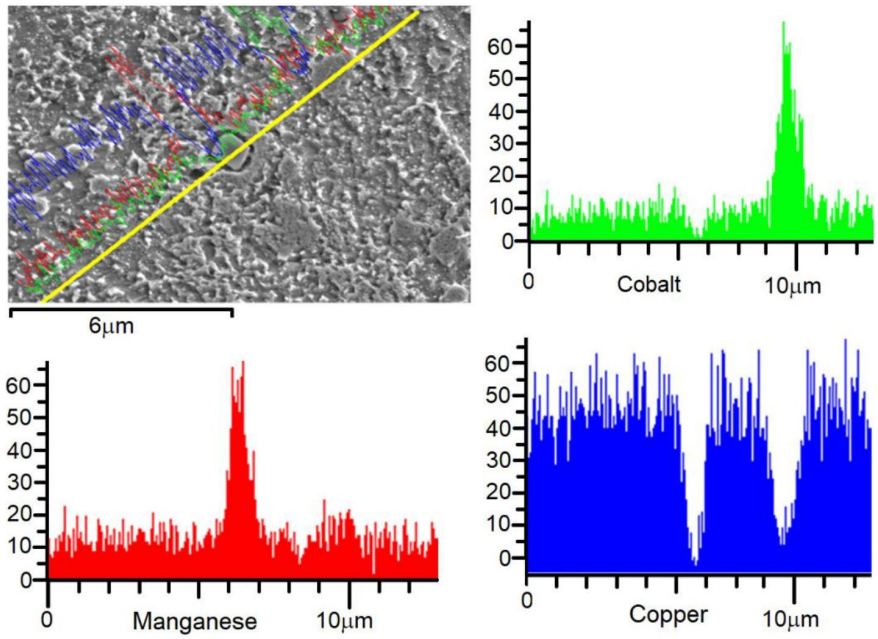

Figure 5. Linear elemental analysis passing through two precipitates.

3.2. Hardness Evaluation

Because metallic parts in machinery are exposed to a constant contact, then, hardness is a parameter that can be controlled to increase the period of useful life of the components, therefore, an evaluation of this mechanical property in the alloys in as-cast condition and after thermal treated was carried out. In Figure 6 are shown the plots of the hardness tests performed on the untreated and treated samples; in the case of M1 sample, without heat treatment a hardness value of 137 HV is observed, for M2 sample it gradually increases to 139 HV, while M3 presents a noticeable increment of its hardness value to 157 HVN. This increase in hardness is attributed to the lattice disorientation between the copper-rich matrix and the second precipitated phase, where evidently, there is no coherence between both phases (different plane orientation) [18], so the plastic flow is inhibited. On the other hand for heat-treated samples, M1 sample shows a hardness value of 122 HV compared to the treated M2 sample with a value of 133 HV resulted to be slightly smaller, while M3 sample shows a hardness increase to 136 HV, then, it is observed that this alloy exhibits a 12.6% increase compared to the treated M1 sample both with thermal treatment. A similar increment occurs for the untreated M3 sample, with a 12.55% increase compared to the treated M1sample. This increase in hardness can be attributed to the formation of the observed precipitates in Figure 1, which were produced after heat treatment [18] [19], allowing the dislocation movement in a lower degree than in as-cast samples. Also is observed for the

three compositions a small reduction of the hardness in this thermal treated alloys compared with the untreated samples, which implies for consequence an increment in the plastic flow [20] [21].

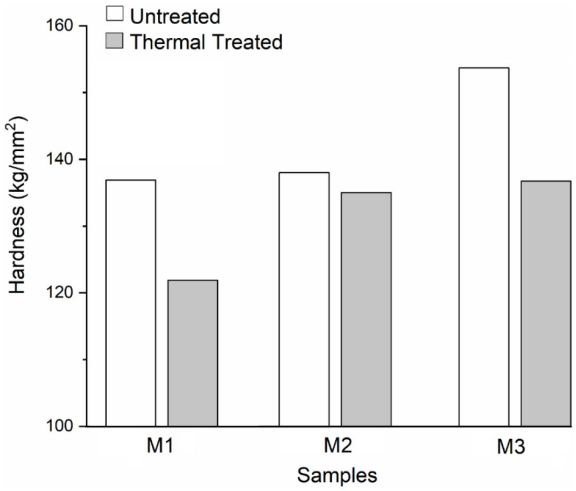

Figure 6. Shows a plot of the hardness values of the untreated M1 sample and the treated M1 sample.

3.3. Tribological Analyses

3.3.1. Weight Losses Evaluation

Weight loss analysis of the samples without heat treatment is presented in **Figure 7**, where is observed that M2 sample showed a notorious wear resistance up to one thousand meters where a stable plateau is observed, after this distance a pronounced weight loss is observed, for this sample an oxidative-adhesive mechanism is observed. In the case of M3 sample a mixed mode between oxidative an abrasive wear mechanism is observed, while M1 sample presents a generalized abrasive wear mechanism. These weight losses are reached when particles produced from the surface sample and the counterpart (which has greater hardness) destroy and remove the produced oxide layer during the friction between both parts of the system in debris form and after a certain period of time; then, these are detached from de worn interface [22].

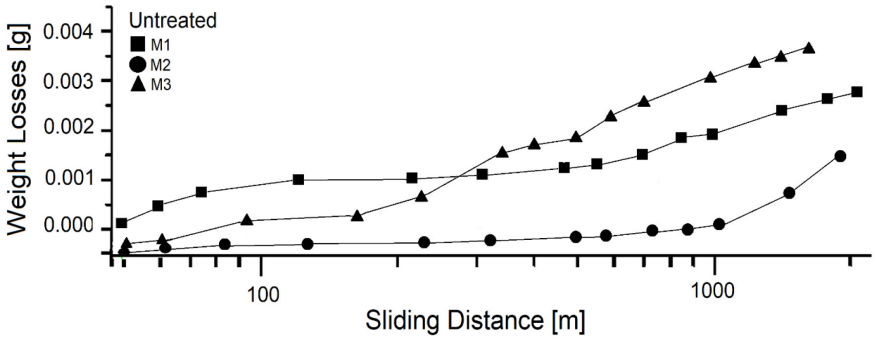

Figure 7. Weight losses as a function of sliding distance of Cu-Co-Mn alloys without treatment.

On the other hand in Figure 8 are presented the wear curves of the weight loss for samples thermal treated heat-treated, where is observed that samples M2 and M3 samples presented similar behavior up to 800 meters, this wear resistance is due to the surface hardness similar of both samples, after this sliding distance M2 sample suffers significant weight loss where a oxide layer depletion is produced; while M3 sample presents an stable plateau after this distance and until the end of the test, these positive behavior is attributed to the formation of an oxide layer due to the friction heating produced between the sample and the counterpart [22] [23].

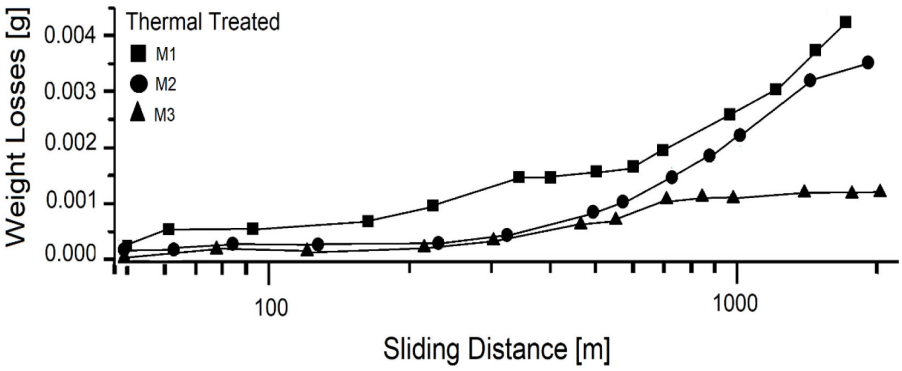

Figure 8. Weight losses as a function of the sling distance of heat-treated Cu-Co-Mn alloys.

3.3.2. Wear Factor Analysis

Because wear in a material is defined as the weight loss and is evaluated as a function of time and/or sliding distance under an applied load and in relative motion, hence, is important to evaluate this tribological process to predict the service life of a component regardless of the type of mechanism involved [22]. One indicative that supports the interpretation of this weight loss phenomenon is the wear factor, which describes the wear tendency of the analyzed system, that is, the amount of weight lost over a certain sliding distance. The results of this process for the heat-treated and untreated samples are presented in Figure 9, which shows the wear factor graph obtained from the wear curves of the evaluated samples. For M1 sample, the untreated sample exhibits a considerably higher wear factor, approximately 65% higher than the treated sample, being this sample with the highest regime of weight losses, due to the low hardness presented in both conditions. On the other hand, M2 sample without thermal treatment shows a 50% higher wear factor than the treated sample, but significantly lower than M1 sample, these reduction in wear factor is attributed to the incorporation of manganese in the structure of the alloy. For the highest content of manganese is observed in the M3 sample shows a similar value, in both conditions, showing a noticeable reduction in their wear factor which is an indicative of the increment in wear resistance produced for the strengthening of the alloy for the incorporation of the manganese. These results obtained clearly indicate the advantage of applying a treatment, where an acceptable value is reached in the wear factor, consequently, a reduction in wear of the alloys is reached [23] [24].

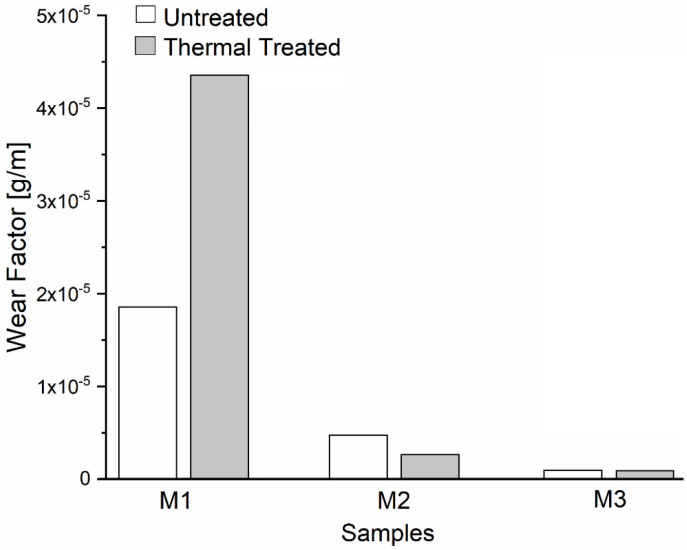

Figure 9. Wear factor of the samples without heat treatment and heat-treated samples.

3.3.3. Worn Surfaces Analyses

In **Figure 10(a)-(c)** are presented the worn surfaces of samples M1, M2 and M3 respectively, with thermal treatment. In **Figure 10(a)** is observed the worn surface of M1 sample which presents predominantly a severe wear, identified by the deep scratches along the observed surface, this type of wear is associated with an abrasive wear mechanism where the counterpart presents much greater hardness than the worn sample, produces this type of morphology. On the other hand, **Figure 10(b)** shows the worn surface of M2 sample, where the appearance of oxides on the surface can be observed, which are produced by the heating by friction between the worn sample and the steel counterpart. It is also possible to observe some wear lines characteristic of abrasive wear, so that in this sample the mechanism is a mixture of abrasive-oxidative which produces a wear not as severe as in the previous sample. The worn surface of the M3 sample is presented in **Figure 10(c)**, where a fully oxidized surface is observed, which is produced because this sample presents an increase in hardness and therefore the resistance to being worn increases, producing excessive heating on the wear interface which produces the generation of oxides that act as a lubricating film between the contact surfaces, thus decreasing the wear of the sample [22]-[24].

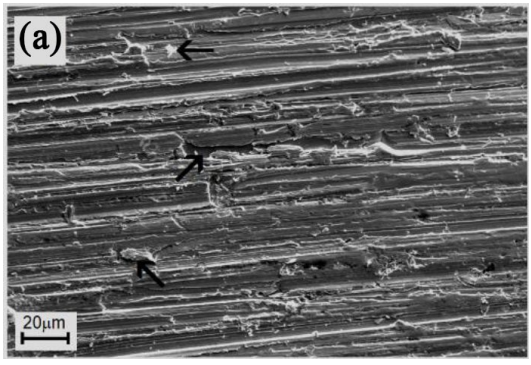

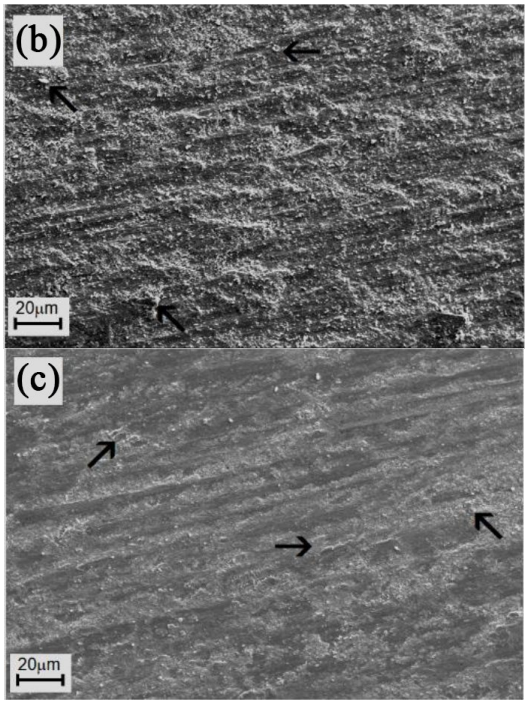

Figure 10. (a) to (c) worn surfaces of samples M1, M2 and M3 respectively, with thermal treatment.

4. Conclusions

Cu-Co based alloys with Manganese additions were obtained successfully by means of melting in an electromagnetic induction furnace and posteriorly thermal treated. Hence the following conclusions are obtained:

- Microstructures obtained in samples thermal treated with the increment in manganese addition have shown a slight reduction in their grain size of approximately 4.5 μm each 5 at.% Mn additions, while porosity ranges lies on the order of 3.2 percent average, being an important parameter to obtain a favorable control of weight losses.
- Hardness results indicated an important increment of 12% in untreated samples with high Manganese content compared with treated samples, being the main cause of this increment the lattice distortion produced by Mn additions, inhibiting the dislocation mobility while treated samples have shown a diminishing in hardness value due to the structure homogenization with the consequent defect reduction.
- Increment in wear resistance was obtained in samples thermally treated and with high manganese content, which is attributed to the formation of a stable oxide layer under an oxidative-adhesive mechanism.

These results were expected to produce an alloy for be used as structural component to resolve some problems in the aeronautic industry.

Acknowledgements

The authors want to thank JL. Roman-Zubillaga for his support in mechanical

characterization. This project was supported under Prodep-UAEM-074.

Conflicts of Interest

The authors declare no conflicts of interest regarding the publication of this paper.

References

[1] Zuo, S., Xiao, F. and Fukuda, T. (2019) Orientation Dependence of Damping Behavior in a Mn-Cu Shape Memory Alloy. *Scripta Materialia*, **170**, 95-98. https://doi.org/10.1016/j.scriptamat.2019.05.042

[2] You, W., Zhang, S., Xu, Y., Deng, M., Xu, X. and Zeng, Q. (2021) Effect of Semi-Solid Solution and Aging on Microstructure and Properties of Mn-Cu Alloy, Rare Met. *Rare Metal Materials and Engineering*, **50**, 979-987.

[3] Zhao, C., Yang, J., Li, G. and Wang, Z. (2022) Laser Powder Bed Fusion of the Mn-Cu Alloys: Printability, Microstructure, and Mechanical Properties. *Journal of Alloys and Compounds*, **899**, Article ID: 163385. https://doi.org/10.1016/j.jallcom.2021.163385

[4] Ma, C.H., Wang, C., Shen, T., Hu, J. and Liang, J. (2020) Properties of M2052 Mn-Cu Alloy Powder Prepared by VIGA Method and Its SLM Prints. *Heat Treatment of Metals*, **46**, 140-147.

[5] Liu, Y., Liang, B., Ye, Z. and Zhang, Y. (2022) Microstructure and Mechanical Properties of Mn-Cu Based Damping Alloy Fabricated by Laser Melting Deposition. *Journal of Physics*: *Conference Series*, **2338**, Article ID: 012051. https://doi.org/10.1088/1742-6596/2338/1/012051

[6] Zhao, C., Deng, H. and Wang, Z. (2023) Microstructure and Strength-Ductility Synergy of Carbon Nanotubes Reinforced Mn-Cu Alloy Composites via Laser Powder Bed Fusion. *Materials Science and Engineering*: *A*, **865**, Article ID: 144658. https://doi.org/10.1016/j.msea.2023.144658

[7] Ma, C., Huang, K., Wang, C., Liu, C., Liu, Z. and Chen, Z. (2025) Effect of Heat Treatment on Microstructure and Damping Properties of MnCu-Based Damping Alloy Prepared by Laser Powder-Bed-Fusion (LPBF). *Materials Science and Engineering*: *A*, **927**, Article ID: 148050. https://doi.org/10.1016/j.msea.2025.148050

[8] Yan, K., Lin, Z., Chen, M., Wang, Y., Wang, J. and Jiang, H. (2022) Fabrication of Mncunife-Cualnifemn Gradient Alloy by Laser Engineering Net Shaping System. *Materials*, **15**, Article 2336. https://doi.org/10.3390/ma15062336

[9] Fan, W., Zhang, C., Tan, H., Wang, Y., Peng, Y., Zhang, F., *et al.* (2022) Microstructures and Mechanical Properties of Invar/MnCu Functionally Graded Material Fabricated by Directed Energy Deposition. *Materials Science and Engineering*: *A*, **860**, Article ID: 144332. https://doi.org/10.1016/j.msea.2022.144332

[10] Tsuchiya, K., Kawabata, O., Umemoto, M., Sato, H. and Marukawa, K. (2000) Aging Response of Shape Memory Behavior in γ-MnCu Alloys. *Materials Science Forum*, **327**, 469-472. https://doi.org/10.4028/www.scientific.net/msf.327-328.469

[11] Shi, S., Liu, C., Wan, J.F., Zhang, J.H. and Rong, Y.H. (2018) Thermodynamic Study of FCC-FCT-FCO Multi-Step Structural Transformation in Mn-Ni Antiferromagnetic Shape Memory Alloys. *Journal of Alloys and Compounds*, **747**, 934-945. https://doi.org/10.1016/j.jallcom.2018.03.052

[12] Shimizu, K., Okumura, Y. and Kubo, H. (1982) Crystallographic and Morphological Studies on the *FCC* to *FCT* Transformation in Mn-Cu Alloys. *Transactions of the Japan Institute of Metals*, **23**, 53-59. https://doi.org/10.2320/matertrans1960.23.53

[13] Yin, F., Sakaguchi, T., Zhong, Y., Sakurai, A. and Nagai, K. (2007) EBSD Characterization of the Twinning Microstructure in a High-Damping Mn-Cu Alloy. *Materials Transactions*, **48**, 2049-2055. https://doi.org/10.2320/matertrans.ma200707

[14] Tian, Q., Yin, F., Sakaguchi, T. and Nagai, K. (2006) Reverse Transformation Behavior of a Prestrained MnCu Alloy. *Acta Materialia*, **54**, 1805-1813. https://doi.org/10.1016/j.actamat.2005.12.007

[15] Jiang, Z.C., Zhang, S.B., Tian, Q.C., Ji, P.G. and Yin, F.X. (2020) Phenomenological Representation of Mechanical Spectroscopy of High Damping Mncunife Alloy. *Materials Science and Technology*, **36**, 743-749. https://doi.org/10.1080/02670836.2020.1738057

[16] Nosova, G.I. (2012) Structurally Inhomogeneous FCT-Martensite in Alloys Based on the Mn-Cu System: Structure, Strain Mechanism and Strength Characteristics. *Metal Science and Heat Treatment*, **54**, 113-117. https://doi.org/10.1007/s11041-012-9464-9

[17] Lu, F., Wu, B., Zhang, J., Li, P. and Zhao, D. (2016) Microstructure and Damping Properties of Mncunifece Alloy. *Rare Metals*, **35**, 615-619. https://doi.org/10.1007/s12598-016-0702-y

[18] Zhang, C., Yang, W., Zhou, R., Xiao, X., Gao, W., Li, Q., *et al.* (2025) Precipitation Characteristics and Microstructure Analysis of a Cu-Mn-Co-P Alloy with High Strength and High Conductivity. *Materials Science and Engineering*: *A*, **923**, Article ID: 147758. https://doi.org/10.1016/j.msea.2024.147758

[19] Hakamada, M., Nakamoto, Y., Matsumoto, H., Iwasaki, H., Chen, Y., Kusuda, H., *et al.* (2007) Relationship between Hardness and Grain Size in Electrodeposited Copper Films. *Materials Science and Engineering*: *A*, **457**, 120-126. https://doi.org/10.1016/j.msea.2006.12.101

[20] Sui, F. and Sandström, R. (2018) Creep Strength Contribution Due to Precipitation Hardening in Copper-Cobalt Alloys. *Journal of Materials Science*, **54**, 1819-1830. https://doi.org/10.1007/s10853-018-2922-z

[21] Bachmaier, A., Rathmayr, G.B., Schmauch, J., Schell, N., Stark, A., de Jonge, N., *et al.* (2018) High Strength Nanocrystalline Cu-Co Alloys with High Tensile Ductility. *Journal of Materials Research*, **34**, 58-68. https://doi.org/10.1557/jmr.2018.185

[22] Kim, K.N., Kim, B.S., Shin, G.S., Park, M.C., Lee, D.H. and Kim, S.J. (2011) Wear Behavior of Self-Lubricating Fe-Cr-C-Mn-Cu Alloys: Smearing Effect of Second Phase Particles. *Metals and Materials International*, **17**, 587-592. https://doi.org/10.1007/s12540-011-0809-5

[23] Gui, M., Kang, S.B. and Lee, J.M. (2000) Dry Sliding Wear Behavior of Spray Deposited Alcumn Alloy and AlCuMn/SiCp Composite. *Journal of Materials Science*, **35**, 4749-4762. https://doi.org/10.1023/a:1004862409233

[24] Qin, Z., Kang, N., Li, R., Zhang, W. and El Mansori, M. (2025) Microstructure and Wear Behavior of Mn-Modified High-Strength Al Cu Alloy Fabricated via Laser Powder Bed Fusion. *Tribology International*, **208**, Article ID: 110660. https://doi.org/10.1016/j.triboint.2025.110660